Quantifying Imported Fire Ant (Hymenoptera: Formicidae) Mounds with Airborne Digital Imagery

JAMES T. VOGT[1]

USDA–ARS Biological Control of Pests Research Unit, P.O. Box 67, Stoneville, MI 38776

Environ. Entomol. 33(4): 1045–1051 (2004)

ABSTRACT Airborne multispectral digital imagery was used to detect imported fire ant mounds in northeast Mississippi pasture. Images were acquired using a GeoVantage GeoScanner camera system, flown at an altitude of 610 m, for a resolution of 0.25 m, and 305 m, for a resolution of 0.1 m. Images were obtained during May 2002, August 2002, November 2002, and February 2003. Distinct mound signatures could be seen in images from May, November, and February; August images were difficult to interpret. Many mounds appeared as dark or light spots of bare soil surrounded by a halo of vigorous vegetation. Up to 75% of mounds were visible in false color infrared images. Mound characteristics (area, height, activity, percent vegetation cover) and image characteristics (image color, spatial resolution) all affected mound detection for at least one sampling period. Increasing spatial resolution from 0.25 to 0.1 m did not affect mound detection in May; during other times of the year, increased resolution improved detection by ≈38%. False color infrared images were generally superior to true color images for mound detection. Potential overestimation because of commission errors was 17–29%.

KEY WORDS multispectral, remote sensing, mounds

IMPORTED FIRE ANTS (red imported fire ant, *Solenopsis invicta* Buren; black imported fire ant, *Solenopsis richteri* Forel; and their hybrid, *Solenopsis invicta* X *richteri*) are serious pests in the southeastern United States, sometimes reaching population densities of 470 mounds (nests)/ha[1] (polygyne *S. invicta*) (Macom and Porter 1996). Fire ants can displace native ants and other invertebrates and attack young animals, and their stinging behavior can interfere with recreational activities of humans (Vinson 1997). Hypersensitive persons who are stung can suffer hospitalization or even death (Rhoades et al. 1989).

Imported fire ants continue to expand into previously uninfested areas, recently appearing in California (Jetter et al. 2002). Isolated infestations north of the general zone of infestation are occasionally noted (e.g., in Oklahoma; personal observation). Determining the extent and density of these infestations presents difficulties in terms of sampling, access to areas over land, and person-hours. Imported fire ants continue to expand their range in North America, with much of the west coast, the east coast north to Maryland, and areas north of the general infestation throughout the southeastern United States at risk (Korzukhin et al. 2001).

Large scale, areawide management programs for imported fire ants require reliable sampling methods, to assess effectiveness of treatments, and long-term changes in fire ant population density. Previous work using aerial photography with color, monochrome infrared, and color infrared film to detect imported fire ant mounds was successful in detecting up to 79.4% of colonies in an area (Green et al. 1977). December was the best time for mound detection. Mound visibility was affected by seasonal mound building activity and changes in vegetation covering mounds. The authors noted a dark spot–red halo signature, caused by low near-infrared (NIR) reflectance from fresh soil excavated by the ants surrounded by highly reflective, lush vegetation immediately surrounding mounds. Leaf-cutting ants have also been the subject of previous work on film-based remote detection of ant colonies [*Atta vollenweideri* Forel (Jonkman 1979) and *Atta texana* (Buckley) (Hart et al. 1971)]. Despite the obvious difficulties and expense involved in detecting and quantifying imported fire ants on the ground, no other published work on remote sensing for fire ant mounds is available.

Developments in remote sensing hardware and software now allow for high-resolution (0.1–0.25 m) airborne digital imagery and have reduced the need to manually georectify and mosaic images of large areas. Sophisticated global positioning systems (GPS), with sub-meter accuracy, allow precise mapping of small targets. These advancements allow for relatively inexpensive, quick delivery, high-resolution imaging of

Mention of trade names or commercial products in this publication is solely for the purpose of providing specific information and does not imply recommendation or endorsement by the U. S. Department of Agriculture.

[1] E-mail: jvogt@ars.usda.gov.

very large areas and rapid collection of accurate ground truth data. A study was conducted to test the feasibility of using such a system to detect and quantify imported fire ant infestations. In this paper, we address effects of mound characteristics that might influence detection (mound area, mound height, percent vegetation cover, and mound activity) and image characteristics (spatial resolution, color) in Mississippi pasture using photointerpretive techniques. While photointerpretation is inherently subjective, it is the simplest analysis method available to anyone with access to basic image viewing software and knowledge of the general appearance of fire ant mounds. Green et al. (1977) provide a description of the appearance of mounds in true color and false color infrared photographs. Digital imagery is playing an increasingly important role in aerial survey and remote sensing, but spatial resolution of digital images is a limiting factor for the detection of small targets; thus, it was necessary to conduct an experiment to compare this newer technology with earlier, film-based work. Classical remote sensing techniques, such as vegetation indices and other band ratios, are useful as tools for highlighting and detecting mounds (unpublished data) but are beyond the scope of this paper and will be reported elsewhere.

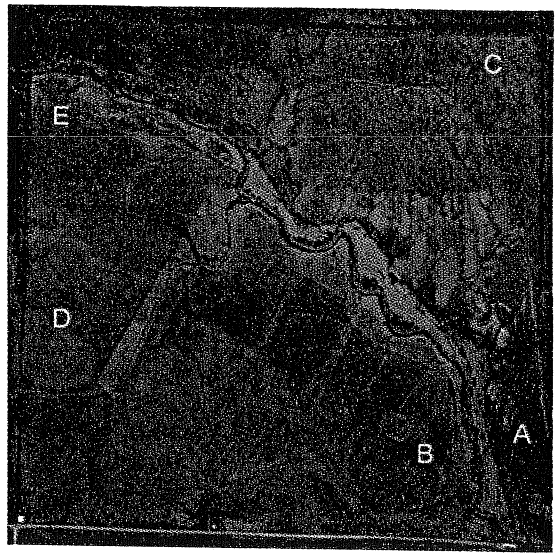

Fig. 1. True color composite image of study site in Clay Co., MS. Image was taken February 2003 at an altitude of 600 m, for a spatial resolution of 0.25 m. Sampling took place in areas marked A, B, and C in May 2002 and all marked areas in August 2002, November 2002, and February 2003. Contains material copyright of GeoVantage, 2003.

Materials and Methods

The site was a large (≈263 ha), grazed pasture in Clay County, MS (≈88°35′15″ W, 33°40′21″ N). The predominant fire ants (and predominant formicids overall) in the pasture were black and hybrid imported fire ants: *S. richteri* Forel and *S. invicta* X *richteri* respectively. Vegetation was primarily Bermuda grass (*Cynodon dactylon* L. Pers.), with mixed grasses and forbs, and patches of browse. A large (100–250 m wide) riparian buffer ran through the area from northwest to southeast. A range of vegetation, soil types, slopes, and elevations occurred throughout the area. Five areas within the pasture were sampled (Fig. 1). East of the riparian buffer (Fig. 1A), moderate slope provided drainage, and vegetation was relatively sparse because of frequent disturbance by cattle congregating at a feeding station located in the area. West of the buffer (Fig. 1B), there was little or no slope and lush vegetation. In the northeastern part of the pasture (Fig. 1C), soil was relatively dry and light in color, and in the far western part of the pasture, we sampled an area of high elevation (Fig. 1D) and a low area that flooded occasionally and contained a high proportion of forbs (Fig. 1E). Areas A, B, and C were included in the initial May samples; D and E were added during subsequent sampling periods. The pasture contained a mixture of clay prairie bottom soils (catalpa-griffith) and mixed prairie bottom soil (leeper). These soils range from very dark grayish brown (catalpa and leeper) to dark olive gray (griffith) when moist.

Imagery was obtained by Geodata Airborne Mapping and Measurement (Macon, MS) at an altitude of 610 m, for a resolution of 0.25 m. For comparison, additional data were obtained at an altitude of 305 m (0.1-m resolution) over a portion of the site on each date. A GeoScanner camera system (GeoVantage, Swampscott, MA), mounted on a Cessna 172 aircraft, consisted of four discrete monochrome digital cameras with 10-nm band-pass filters (450, 550, 650, and 850 nm). A GPS antenna and 12-channel receiver were installed on the plane and integrated with the data collection system, and an Inertial Measurement Unit (IMU) provided acceleration and rotation rates for the camera axes. Proprietary software (GeoVantage) was used to georegister and mosaic individual images. Data from each flight were delivered as two georeferenced true color (RGB) and false color infrared (NIR) mosaics, along with individual georeferenced frames. Imagery was acquired during the following times: May 2002, August 2002, November 2002, and February 2003. The only image processing applied after delivery of the mosaics was a 2% linear histogram stretch (ENVI, Research Systems, Boulder, CO), which served to increase contrast.

Images were examined for suspected fire ant mounds using photointerpretation. For the primary research site, plots ($N = 20$, with the exception of May 2002, $N = 21$), ≈4 ha each and scattered throughout the areas indicated in Fig. 1, were overlaid onto the image, and suspected mounds were marked. Mound locations on the ground were determined within 2 wk of data capture. GIS data were gathered using a Starlink Invicta 210 DGPS/Beacon Receiver (Starlink, Austin, TX) and recorded in SoloField CE (Tripod Data Systems, Corvallis, OR). A pair of workers searched each plot thoroughly for fire ant mounds. The area of each mound located within a plot was measured. Because fire ant mounds tend to be ellip-

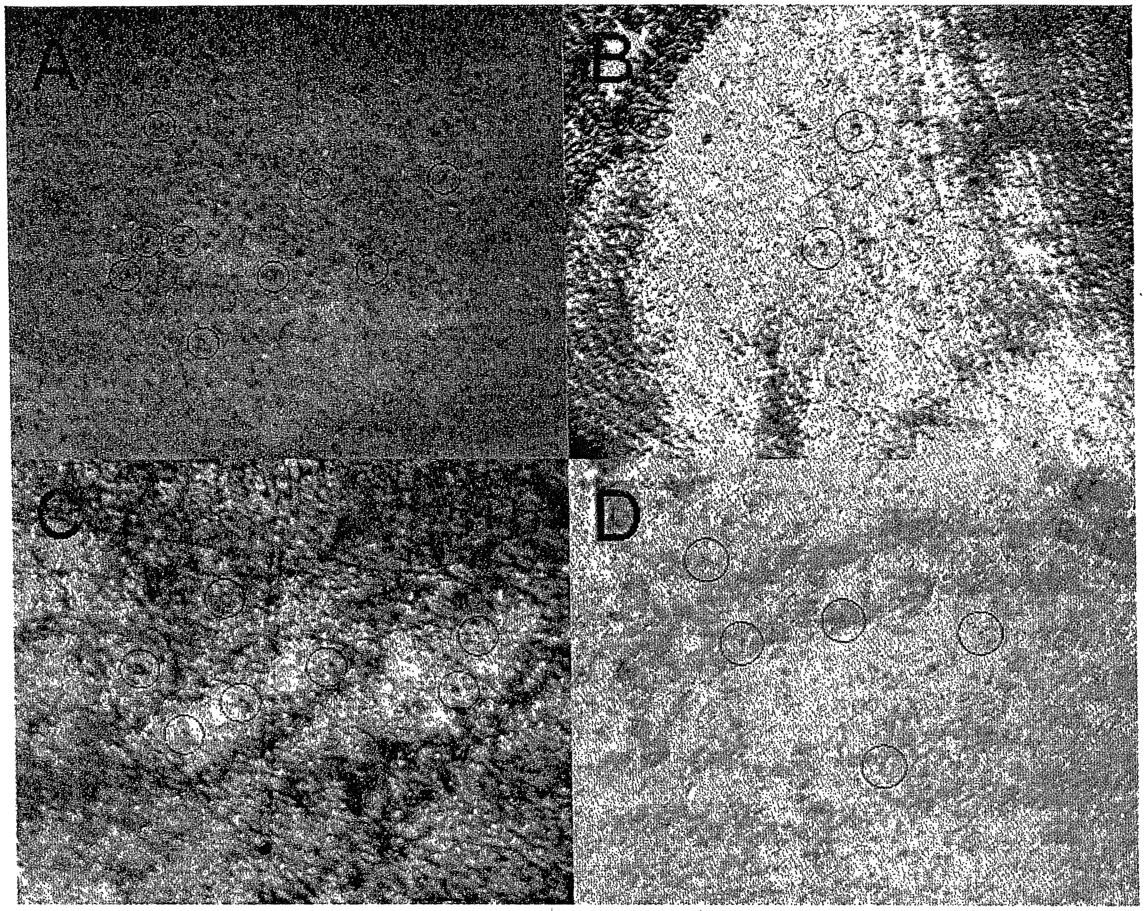

Fig. 2. Examples of imported fire ant mounds in airborne digital images of Mississippi pasture. Images are false color infrared composites obtained in May 2002 at 0.1-m resolution (A and B), in February 2003 at 0.25-m resolution (C), and August 2002 at 0.25-m resolution. Not all mounds are circled. Contains material copyright of GeoVantage, 2002 and 2003.

tical (Hubbard and Cunningham 1977), each mound was measured along its longest aspect and narrowest aspect. Mound size was expressed as area, using the equation Area = $\pi \times a \times b$, where a is the semimajor axis and b is the semiminor axis. Percent of the mound covered with emergent vegetation was estimated. Each mound was designated active (y) or inactive (n) by probing and looking for emergence of disturbed worker ants. Each mound was georeferenced and assigned a unique number.

Data were first examined to determine whether conditions were met for normal approximation to a binomial distribution; because of sufficient numbers (range, 398–749), analyses were conducted assuming normal distribution of predicted mean values. Data were analyzed as a split-plot using Proc Mixed (Littell et al. 1996), with mound activity as the main unit (active versus inactive), and resolution (0.25 and 0.1 m) and color (NIR and RGB) as subunits. Plot was used as a block effect. Data were analyzed by date to determine which factors (resolution, color, mound activity) were most important for mound detection. Commission errors were analyzed using Proc Mixed to determine the effects of date and image color. Mound size, mound height, mound volume, and vegetation cover were added to the model individually for each date, allowing a linear trend for probability of detecting a mound as a function of each variable.

Results

The characteristic appearance of mounds in the images varied throughout the year and was not consistent between sampled areas in the pasture. In NIR composites, mounds appeared as black or dark brown spots surrounded by a red ring or "halo" of vegetation (May, November, and February, area B in pasture; Fig. 2A), as light spots surrounded by a red halo (May, November, February, and to a lesser degree in August, areas A, C, and D in pasture; Fig. 2B), as dark or light spots with a less distinct ring (all dates, area E in pasture; Fig. 2C), or as faint red spots, sometimes with a halo evident, because of mounds being mostly overgrown with vegetation (August, all areas; Fig. 2D). The halo, when present, was generally dark green in RGB composites.

Table 1. Least squares means for percent of black and hybrid imported fire ant mounds detected in airborne digital images of Mississippi pasture

Effect	Mound activity[a]	Image color[b]	Image resolution (m^2)	Percent mounds detected ± SE[c]			
				May	August	November	February
Mound activity	N	—	—	47 ± 4b	20 ± 5b	41 ± 8a	36 ± 7a
Mound activity	Y	—	—	61 ± 4a	31 ± 5a	45 ± 8a	46 ± 7a
Resolution	—	—	0.1	54 ± 4a	34 ± 5a	51 ± 8a	49 ± 7a
Resolution	—	—	0.25	54 ± 3a	17 ± 4b	36 ± 8b	32 ± 6b
Image color	—	NIR	—	62 ± 4a	33 ± 5a	51 ± 8a	42 ± 7a
Image color	—	RGB	—	46 ± 4b	19 ± 5b	35 ± 8b	39 ± 7a
Activity × color	N	NIR	—	52 ± 5b	26 ± 5b	49 ± 8a	36 ± 8a
Activity × color	N	RGB	—	42 ± 5b	15 ± 5c	33 ± 8b	36 ± 8a
Activity × color	Y	NIR	—	72 ± 5a	40 ± 5a	53 ± 8a	49 ± 8a
Activity × color	Y	RGB	—	50 ± 5b	22 ± 5b	38 ± 8b	43 ± 8a

[a] N, inactive mounds; Y, active mounds.
[b] NIR, false color infrared composite; RGB, true color composite.
[c] Means within a combination of effects followed by the same letter are not significantly different (least squares means, $P > 0.1$).

The highest overall percentage of active fire ant mounds detected during the study was 75% (May, NIR image at 0.1-m resolution), although detection rates in individual plots sometimes approached 100% at 0.1- and 0.25-m resolution. An examination of variances for all possible date × image resolution × color combinations between areas within the pasture revealed no detectable trends; therefore, area was treated as a random source of error in further analyses. Likewise, an F-test for interactions between area within the pasture and mound activity, image resolution, and image color revealed no potential interactions ($P > 0.05$). The relative importance of these factors for mound detection was determined using Proc Mixed, with mound activity, resolution, color, and their interactions as fixed effects. Estimated least squares means for significant effects are summarized in Table 1. In May, image color was the most important factor for mound detection ($F = 24.3$, df = 1,54, $P < 0.0001$), followed by mound activity ($F = 5.23$, df = 1,52, $P = 0.0264$), and the mound activity × color interaction ($F = 4.0$, df = 1,54, $P = 0.051$). In August, image resolution, color, and mound activity influenced mound detection ($F = 29.7$, df = 1,84, $P < 0.0001$, $F = 28.0$, df = 1,80, $P < 0.0001$ and $F = 7.7$, df = 1,36.1, $P = 0.0088$, respectively). In November, color and image resolution influenced mound detection ($F = 31.0$, df = 1,79, $P < 0.0001$ and $F = 20.6$, df = 1,83, $P < 0.0001$, respectively), and in February, only image resolution had a significant effect ($F = 22.1$, df = 1,77, $P < 0.0001$).

Commission errors (marking an area on an image as a mound where there is no mound present) varied with date and image color ($F = 7.6$, df = 3,8, $P = 0.0203$ and $F = 11.4$, df = 1,23, $P = 0.0027$, respectively). In general, commission errors were slightly lower when interpreting NIR images. Data are summarized in Table 2.

Next, to examine the effect of mound area (m^2) on detection and determine the mound and sampling conditions that would offer the greatest probability of detecting mounds for each sampling date, area was added to the model as a covariate and allowed to interact with mound activity, image resolution, and color. In May, mound area positively influenced mound detection ($F = 108.2$, df = 1,938, $P < 0.0001$), and there was a significant area × mound activity interaction ($F = 84.4$, df = 2,771, $P < 0.0001$); increas-

Table 2. Potential overestimation caused by commission errors for imported fire ant mound detection in multispectral airborne digital images

Effect	Image color[a]	Date	Mean number of false positives/plot[b]	Mean number of mounds/plot	Percent overestimation
Date	—	May	4.8 ± 1.6b	23.9 ± 2.1	20.0
Date	—	August	3.7 ± 1.3b	20.0 ± 7.3	18.5
Date	—	November	8.6 ± 1.3a	37.2 ± 16.6	23.1
Date	—	February	8.5 ± 1.3a	34.4 ± 14.8	24.7
Image color	NIR	—	5.6 ± 1.1b	28.8 ± 14.3	19.4
Image color	RGB	—	7.2 ± 1.1a	28.8 ± 14.3	25.0
Date × image color	NIR	May	4.1 ± 1.7bc	23.9 ± 2.1	17.2
Date × image color	RGB	May	5.5 ± 1.7bc	23.9 ± 2.1	23.0
Date × image color	NIR	August	3.9 ± 1.4c	20.0 ± 7.3	19.5
Date × image color	RGB	August	3.4 ± 1.4c	20.0 ± 7.3	17.0
Date × image color	NIR	November	7.4 ± 1.4b	37.2 ± 16.6	19.9
Date × image color	RGB	November	10.0 ± 1.4a	37.2 ± 16.6	26.9
Date × image color	NIR	February	7.0 ± 1.4b	34.4 ± 14.8	20.3
Date × image color	RGB	February	9.9 ± 1.4a	34.4 ± 14.8	28.8

[a] NIR, false color infrared composite; RGB, true color composite.
[b] Means within a combination of effects that are followed by the same letter are not significantly different (least squares means, $P > 0.1$).

Table 3. Regression statistics for the relationship between imported fire ant mound area and mound height for active and inactive mounds

Date	x^a	y^b	Mound activity	Intercept ± SE[c]	Slope ± SE	df	t	P
May	Mound area	Mound height	Active	13.9 ± 2.2	37.7 ± 2.0	495	18.6	< 0.0001
			Inactive		11.8 ± 1.9	495	−13.3	< 0.0001
August	Mound area	Mound height	Active	12.9 ± 0.9	40.9 ± 2.6	386	15.6	< 0.0001
			Inactive		17.6 ± 2.2	390	−10.6	< 0.0001
November	Mound area	Mound height	Active	12.4 ± 1.0	44.3 ± 2.3	507	19.2	< 0.0001
			Inactive		33.2 ± 4.8	8	−2.3	0.0469
February	Mound area	Mound height	Active	12.1 ± 0.9	38.7 ± 2.1	418	18.3	< 0.0001
			Inactive		23.6 ± 4.0	12	−3.8	0.0027

[a] Area is in m^2.
[b] Height is in cm.
[c] Intercepts ≠ 0 ($P < 0.05$).

ing mound size had less effect on detection for inactive mounds than for active mounds. In August, mound area also influenced mound detection; mound activity may have had a small effect on the relationship between mound area and detection ($F = 3.7$, df = 1,663, $P = 0.054$). In November, mound area was highly significant ($F = 178.5$, df = 1,1949, $P < 0.0001$); the effect of mound area was decreased for active mounds ($F = 9.8$, df = 1,1898, $P = 0.002$) and increased in the NIR image ($F = 9.6$, df = 1,1451, $P = 0.002$). In February, the effect of mound area was significant ($F = 141.6$, df = 1,1742, $P < 0.0001$) and increased in the NIR image ($F = 4.2$, df = 1,1452, $P = 0.041$).

Mound height explained a significant portion of the variation in mound detection for all sampling dates ($P < 0.0001$). It was suspected that the mound height–mound area relationship would be different for active versus inactive mounds (i.e., the height of abandoned mounds is not maintained by worker ants so they eventually collapse), so data were subjected to Proc Mixed to test for effects of mound area, mound activity, and mound area × mound activity on mound height. Mound activity had no effect on mound height in the model for any date ($P > 0.8$), but the slope of the relationship between mound area and mound height was significantly lower for inactive mounds than active mounds on all sampling dates ($P < 0.05$); this effect was most pronounced in May and August (Table 3). Because mound area and mound height both influenced detection, and the shape of fire ant mounds at our site roughly approximated an ellipsoid sectioned at ground level, an estimate of above ground volume was calculated for each mound using the formula Volume = $0.5 \times (1.3 \times \pi \times a \times b \times c)$, where a is the semimajor axis, b is the semiminor axis, and c is height from ground level. Volume was added to the model in the same manner as mound area and allowed to interact with mound activity, image color, and resolution. In May and August, mound volume was a significant predictor of mound detection ($F = 141.7$, df = 1,991, $P < 0.0001$ and $F = 75.1$, df = 1,878, $P < 0.0001$, respectively). In November, mound volume was highly significant ($F = 215.0$, df = 1,1769, $P < 0.0001$); the effect of mound volume was decreased for active mounds ($F = 14.1$, df 1,1728, $P = 0.0002$) and increased in NIR images ($F = 9.7$, df = 1,1678, $P = 0.0019$). In February, mound volume was highly significant ($F = 135.1$, df = 1,1361, $P < 0.0001$); the effect of mound volume was slightly decreased at higher resolution ($F = 5.2$, df = 1,1831, $P = 0.0224$) and slightly increased in the NIR image ($F = 3.9$, df = 1,1171, $P = 0.0490$).

A range of potential mound volumes (10–100 liters at 10-liter increments) was inserted into the model to determine the likelihood of detecting active mounds of different size in 0.1-m resolution, false color infrared images. Few mounds were >0.6 m^2 in area or 100 liters in volume; mound sizes and associated statistics are given in Table 4. The linear relationships between predicted percent detection and mound volume for each date are illustrated in Fig. 3.

Vegetation cover (estimated percent cover of mound) was added to the model in place of mound volume as a covariate and allowed to interact with mound activity, image resolution, and color. Vegetation cover had no effect on mound detection in May,

Table 4. Mean area and volume of imported fire ant mounds in a Mississippi pasture on four sampling dates

Date	Variable	Mean ± SE[a]	N	Range
May	Area	0.273 ± 0.008	502	0.006–0.918
	Volume	45.1 ± 1.8		0.12–245.6
August	Area	0.225 ± 0.007	399	0.023–0.777
	Volume	32.9 ± 1.4		0.77–141.4
November	Area	0.182 ± 0.005	740	0.008–0.948
	Volume	28.2 ± 1.1		0.25–183.3
February	Area	0.243 ± 0.008	688	0.003–0.816
	Volume	37.7 ± 35.5		0.04–238.8

[a] Area is expressed in m^2 and volume is expressed in liters.

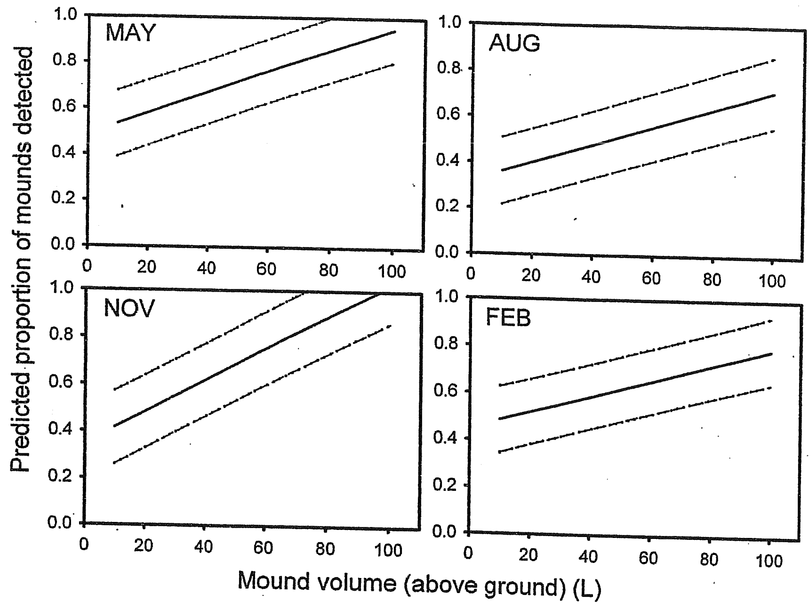

Fig. 3. Regression of estimated proportion of active imported fire ant mounds detected in airborne digital images over mound volume (estimated for false infrared composites, 0.1-m resolution). Estimated regression equations are as follows: May, $y = 0.0046 \pm 0.0004x + 0.488 \pm 0.073$; August, $y = 0.0039 \pm 0.0005x + 0.323 \pm 0.066$; November, $y = 0.0067 \pm 0.0010x + 0.373 \pm 0.72$; February, $y = 0.0034 \pm 0.0005x + 0.453 \pm 0.066$. Broken lines enclose the 95% confidence intervals.

August, or November ($P > 0.3$). In February, detection of inactive mounds increased as vegetation cover increased ($F = 3.9$, df = 1,427, $P = 0.0486$). Setting vegetation cover = 20 and vegetation cover = 60 for the model, predicted detection of inactive mounds rose from 23 ± 8 to 33 ± 7%.

Discussion

Changes in the appearance of imported fire ant mounds throughout the season are a result of differences in mound building activity, primarily driven by environmental conditions (see Best and Drees 2001). Seasonal differences in the average size and condition of imported fire ant mounds are important factors to consider for implementing a remote sensing program for fire ant monitoring and/or detection. In this study, May proved to be the best month for mound detection. Mild temperatures and relatively moist soil conditions during the spring are conducive to mound building activity, and mounds were largest during that period (Table 3). By August, conditions at the study site were very dry, and most mounds lacked the ring of robust vegetation in and around them that was fairly prominent at other times of year. On average, only 34% of mounds were detected in August images. Mound building activity by imported fire ants can be initiated by rain during otherwise dry times of year, and with careful timing of data collection, it might be possible to capture useful imagery during all times of the year. More work is needed to model variation in mound building activity driven by environmental conditions. Other factors may need to be taken into consideration; for example, in November, increasing mound size had a greater positive effect on detection of inactive mounds than active mounds. Active mounds were strongly skewed toward smaller sizes, whereas inactive mounds were relatively evenly distributed (data not shown). This may be because of emergence of young colonies after spring mating flights.

Seasonal trends in mound detection in this study are similar to what Green et al. (1977) observed in Texas coastal plains areas. In their study, winter was the best time to detect mounds. As in this study, detection was lowest in August. The data herein are comparable to theirs in terms of the percentage of mounds detected, although with the limits of resolution for the digital imaging system, slightly fewer mounds were detected during all times of year. Some advantages to using digital imagery rather than photography include less processing time and the ease of postprocessing (e.g., enhancing contrast, displaying different color bands, adjusting scale). Reliable, relatively inexpensive (~\$0.80–1.00/ha) data can be gathered and delivered same or next day, already orthorectified and mosaiced.

Commission errors might vary with photointerpreter; in this study, interpretation of images was not conservative because the intent of the study was to test the limits of the imagery for detection of different sized mounds. Commission errors can be greatly reduced by marking only mounds with a very distinct signature, particularly those with a prominent red halo in NIR composites. Potential overestimation of mound density was generally highest in RGB composites (Table 2), which do not reveal the relatively high reflectance of near infrared light from vigorous vegetation growing within and immediately surrounding mounds.

Data on remote sensing for imported fire ant mounds during different times of the year and under different conditions will form the basis for informed decisions when planning future remote sensing work. Clearly, time of year, image resolution, and image color are important factors to consider. Some of the interactions that surfaced in these analyses will also be helpful for understanding and applying multispectral imagery for fire ant mound detection. In the spring, for example, likelihood of detecting inactive mounds did not increase as quickly with mound size as likelihood of detecting active mounds. Also in the spring, the advantage of using NIR imagery was greater for detecting active mounds than inactive mounds (see Table 1). Additional testing in other areas infested by imported fire ants will be necessary to confirm these trends. Abandoned mounds eventually collapse, reducing the advantages of increased aeration and infiltration to the plants growing in and around them, so the advantage of using NIR imagery for detecting enhanced plant growth in and around mounds would be expected to decrease for inactive mounds.

Data obtained in May (NIR, 0.1-m resolution) seem to offer the greatest chance to reliably predict the percentage of visible mounds based on mound volume (See Fig. 3). Looking at estimated means for the desired combination of effects and calculating the confidence interval for the predicted regression line can easily generate similar data for other conditions. Visually estimating mound length and width in pixels and converting to the desired units can yield an estimated mound size in images. In May, predicted detection success for the average mound size (45 liters, see Table 4) is $\approx 70 \pm 12\%$. Because many factors that may influence mound detection, such as soil and vegetation type, vary between locations, the predictive value of regressions generated using the data herein is limited to a single site. More detailed analyses will be required to take into account commission errors and site differences to produce predictive models with broad applicability.

In conclusion, airborne multispectral digital imagery can be a useful tool for detecting and quantifying imported fire ant mounds in Mississippi pasture. Work in progress is targeted toward testing multispectral imagery as a detection tool in different areas and under different conditions, and additional studies are underway to develop and refine predictive models for estimating fire ant mound density based on detection of larger mounds.

Acknowledgments

I thank J. Davis, A. Martin, E. Gourley, and D. Harsh for assistance in the field. J. Ritchie and S. Sampson provided many helpful suggestions on an earlier version of the manuscript. I also thank D. Boykin for statistical advice and additional suggestions and J. Bryan (Prairie Livestock) for access to his property.

References Cited

Best, R., and B. M. Drees. 2001. Red imported fire ant and weather reporting program: final report 2000–2001. Available online at http://fireant.tamu.edu/research/arr/year/00-02/2000-2002ResDemHbk.htm#weather. Accessed on May 11, 2004.

Green, L. R., J. K. Olson, W. G. Hart, and M. R. Davis. 1977. Aerial photographic detection of imported fire ant mounds. Photogramm. Eng. Rem. Sens. 43: 1051–1057.

Hart, W. G., S. J. Ingle, M. R. Davis, C. Magnum, A. Higgins, and J. C. Boling. 1971. Some uses of infra-red aerial color photography in entomology, pp. 99–113. *In* A. Anson (ed.), Proceedings of the 3rd Biennial Workshop on Aerial Color Photography in the Plant Sciences, Gainesville, FL, American Society of Photogrammetry.

Hubbard, M. D., and W. G. Cunningham. 1977. Orientation of mounds in the ant *Solenopsis invicta* (Hymenoptera: Formicidae: Myrmicinae). Insectes Soc. 24: 3–7.

Jetter, K. M., J. Hamilton, and J. H. Klotz. 2002. Eradication costs calculated: red imported fire ants threaten agriculture, wildlife, and homes. Calif. Agric. 56: 26–34.

Jonkman, J.C.M. 1979. Distribution and densities of nests of the leaf-cutting ant *Atta vollenweideri* Forel, 1983 in Paraguay. Zeitsch. Angew. Entomol. 88: 27–43.

Korzukhin, M. D., S. D. Porter, L. C. Thompson, and S. Wiley. 2001. Modeling temperature-dependent range limits for the fire ant *Solenopsis invicta* (Hymenoptera: Formicidae) in the United States. Environ. Entomol. 30: 645–655.

Littell, R. C., G. A. Milliken, W. W. Stroup, and R. D. Wolfsinger. 1996. SAS system for mixed models. SAS Institute, Cary, NC.

Macom, T. E., and S. D. Porter. 1996. Comparison of polygyne and monogyne red imported fire ants (Hymenoptera: Formicidae) population densities. Ann. Entomol. Soc. Am. 89: 535–543.

Rhoades, R. B., C. T. Stafford, and F. K. James, Jr. 1989. Survey of fatal anaphylactic reactions to imported fire ant stings. J. Allergy Clin. Immunol. 84: 159–162.

Vinson, S. B. 1997. Invasion of the red imported fire ant (Hymenoptera: Formicide). Spread, biology and impact. Am. Entomol. 43: 23–39.

Received 26 June 2003; accepted 23 February 2004.